THE ASTROPHYSICAL JOURNAL, 548:836–851, 2001 February 20
© 2001. The American Astronomical Society. All rights reserved. Printed in U.S.A.

THE ABUNDANCES OF SOLID N_2 AND GASEOUS CO_2 IN INTERSTELLAR DENSE MOLECULAR CLOUDS

S. A. SANDFORD,[1] M. P. BERNSTEIN,[1,2] L. J. ALLAMANDOLA,[1] D. GOORVITCH,[1] AND T. C. V S. TEIXEIRA[3]

Received 2000 August 4; accepted 2000 October 4

ABSTRACT

We present 2338–2322 cm^{-1} (4.277–4.307 μm) infrared spectra of a number of N_2-containing mixed molecular ices and demonstrate that the strength of the infrared "forbidden" band due to the N≡N stretch near 2328 cm^{-1} (4.295 μm) is extremely sensitive to the composition of the ice. The strength of the 2328 cm^{-1} N_2 fundamental is significantly enhanced relative to that of pure N_2 ice when NH_3, H_2O, or CO_2 are present, but it is largely unaffected by the presence of CO, CH_4, or O_2. We use the laboratory data in conjunction with *Infrared Space Observatory* (*ISO*) data that probe several lines of sight through dense molecular clouds to place limits on the abundance of interstellar solid phase N_2 and the composition of the ices. Deriving upper limits is complicated by the presence of overlapping absorptions due to CO_2 gas in the clouds and, in some cases, to photospheric CO in the background star. These upper limits are just beginning to be low enough to constrain interstellar grain models and the composition of possible N_2-bearing interstellar ices. We outline the search criteria that will need to be met if solid interstellar N_2 is to be detected in the future. We also discuss some of the implications of the presence of warm CO_2 gas along the lines of sight to embedded protostars and demonstrate that its presence may help resolve certain puzzles associated with the previously derived gas/solid CO_2 ratios and the relative abundances of polar and nonpolar ices toward these objects. Finally, we briefly comment on the possible implications of these results for the interpretation of N_2 detections on outer solar system bodies.

Subject headings: infrared: ISM: lines and bands — ISM: abundances — ISM: molecules — methods: laboratory — molecular data — techniques: spectroscopic

On-line material: machine-readable table

1. INTRODUCTION

In terms of its distribution and molecular state, nitrogen is the least well understood of the major elements in dense molecular clouds. A number of N-bearing molecular species have been identified in the gas phase in dense clouds via rotational transitions using radio techniques (see van Dishoeck et al. 1993; Irvine 1998), but these molecules only account for a minor fraction of the total cosmic abundance of nitrogen along these lines of sight. At the low temperatures typical of dense molecular clouds ($T < 30$ K), most molecular species should be largely depleted from the gas phase by condensation onto dust grains (Sandford & Allamandola 1993; Sandford 1996; Whittet et al. 1996). Thus, much of the nitrogen in dense clouds probably resides in ice mantles on interstellar grains.

To date, only a few N-bearing molecules have been identified in interstellar ices using infrared spectroscopy. The most abundant of these, ammonia (NH_3), has only recently been unequivocally identified (Lacy et al. 1998). The presence of NH_3 in the ices is not surprising since it is observed to be abundant in the gas phase in dense clouds (see Myers & Benson 1983), and gas-grain chemistry models predict that it should be a major product of H-addition reactions on grain surfaces (Tielens & Hagen 1982; d'Hendecourt, Allamandola, & Greenberg 1985). In the few objects where NH_3-containing ices have been detected to date, the NH_3/H_2O ratio is about 0.1, suggesting that NH_3 in ices accounts for only a small portion of the total available cosmic nitrogen in clouds.

The only other N-bearing species seen in the solid state in dense clouds has yet to be identified unequivocally. The spectra of some protostars embedded in dense clouds contain an absorption feature near 2165 cm^{-1} (4.619 μm; see Lacy et al. 1984; Tegler et al. 1993; Pendleton et al. 1999). This spectral position is characteristic of the C≡N stretching vibration, and the feature can be well matched by C- and N-containing laboratory ice analogs that are exposed to radiation (for recent discussions see Grim & Greenberg 1987; Bernstein, Sandford, & Allamandola 1997, 2000; Palumbo, Pendleton, & Strazzulla 2000a, 2000b). The abundance of this material is difficult to access since its identity and overall distribution are not known. However, there are indications that this band may have a large intrinsic strength (Bernstein et al. 1997), and it is unlikely that the carrier of this weak band can be responsible for more than a minor fraction of the nitrogen in dense clouds. Thus, the currently identified gas- and ice-phase N-bearing molecules leave the majority of the cosmic nitrogen in dense clouds unaccounted for.

There are good reasons for believing that much of the "missing" nitrogen is present in the form of N_2. Interstellar gas-grain chemistry models predict that N_2 should be formed on ice mantles by atom addition reactions under the proper conditions (see Tielens & Hagen 1982; d'Hendecourt et al. 1985; Brown & Charnley 1990; Hasegawa, Herbst, & Leung 1992). In dense cloud environments where H/H_2 is large, gas-surface reactions will be dominated by H atom addition and atoms like C, O, and N will be largely converted to simple hydrides like CH_4, H_2O, and NH_3. If H/H_2 is substantially less than 1, however, reactive

[1] NASA Ames Research Center, Mail Stop 245-6, Moffett Field, CA 94035.

[2] SETI Institute, 2035 Landings Drive, Mountain View, CA 94043.

[3] Institute of Physics and Astronomy, University of Århus, Ny Munkegade, DK-8000 Århus C, Denmark.

species like O and N are free to react with one another to form molecules like O_2 and N_2. N_2 has fully occupied pi orbitals; it is therefore relatively unreactive, and once formed it is likely to remain largely unchanged by further gas-grain reactions (although particle irradiation can alter some of it; see Palumbo et al. 2000a). Thus, two qualitatively different types of ice mantles may be produced by grain surface reactions, one dominated by polar, H-bonded molecules and the other dominated by only slightly polar, highly unsaturated molecules. This basic concept is confirmed by the observation that CO in interstellar ices is found to be frozen in both H_2O- rich polar ices and some form of nonpolar ice (see Sandford et al. 1988; Tielens et al. 1991; Whittet et al. 1996; Elsila, Allamandola, & Sandford 1997; Ehrenfreund et al. 1998a, 1998b; Teixeira, Emerson, & Palumbo 1998).

Since N_2 will be most efficiently formed in regions with low atomic H, the N_2 should be incorporated into ices that are rich in O_2, CO, and CO_2 but that may also contain significant amounts of H_2O and NH_3 (see Tielens & Hagen 1982; d'Hendecourt et al. 1985). Cloud chemistry models predict an enormous range of N_2/H_2O, N_2/NH_3, and N_2/CO_2 ratios depending on assumed densities, H/H_2 ratios, initial atomic abundances, etc. For example, the models described in the two references above yield N_2/H_2O and N_2/NH_3 ratios that range over 6 orders of magnitude and N_2/CO_2 ratios that range over 2 orders of magnitude. Thus, the theoretical expectations for the abundance and distribution of N_2 in interstellar ices are currently poorly constrained.

It should be noted that there is some *indirect* evidence that much of the nitrogen in dense clouds is in the form of N_2. This evidence is based on the observation that some of the best fits in position and profile to the apolar interstellar CO ice feature near 2140 cm^{-1} (4.67 μm), which is most prominent in quiescent regions of dense clouds, are provided by ices dominated by N_2, O_2, and CO_2, with possible contributions from some H_2O (Elsila et al. 1997; Ehrenfreund et al. 1998a, 1998b).

Unfortunately, the *direct* detection of N_2 in the interstellar medium is extremely difficult. As a homonuclear, diatomic molecule, it has no permanent dipole moment and so is not amenable to radio detection in the gas phase. The N≡N stretching vibration at 2328.2 cm^{-1} (4.295 μm) does not induce a change in dipole moment and is therefore infrared inactive in the gas phase. The N≡N stretching vibration is weakly detectable in the solid state, however, because heterogeneous interactions with neighboring molecules induce small dipole moment changes. The strength, or "*A* value," of pure α phase N_2 is about 1.8×10^{-22} cm/N_2, i.e., only about *one hundred thousandth* that of CO (Bohn et al. 1994; Bernstein & Sandford 1999). This makes it extremely difficult to detect directly the absorption of N_2 in interstellar ices, even if this molecule is very abundant. Additionally, since the N≡N stretch falls near 2328 cm^{-1}, it cannot be detected from the ground because of strong absorption produced by telluric atmospheric CO_2. However, this region has become accessible through *ISO*, and data containing potential information about solid molecular nitrogen can now be examined.

Since the N≡N stretching feature in ices is only detectable because it is induced by interactions with neighboring molecules, its intrinsic strength and profile are strong functions of the composition of the other molecules in the ice. Recent laboratory experiments have shown that the strength of the induced feature can be highly variable. In particular, it can be enhanced by factors of 10–1000 over its value in pure N_2 ices by the presence of NH_3, H_2O, or CO_2 (Bernstein & Sandford 1999). Since these other molecules may well exist in the same interstellar ices that are expected to contain N_2, this makes the detection of interstellar N_2-containing ices a considerably more hopeful affair.

In this paper we make a first attempt to use the recent laboratory data to constrain the abundance of N_2 in interstellar ices. In the following sections we will briefly review how the strength and shape of the N_2 stretching fundamental are affected by the presence of other molecules and consider the N_2 band strengths that might be anticipated in interstellar ices (§ 2). We then present the spectra of several objects (W33A, NGC 7538 IRS 9, AFGL 2136, and Elias 16) observed by *ISO* (§ 3) and use the laboratory results to place constraints on the abundances and compositions of N_2-containing ices along the lines of sight to AFGL 2136 and Elias 16 (§ 4). The astrophysical implications of our results are then discussed (§ 5).

2. THE N_2 STRETCHING FUNDAMENTAL

Recent work in the Ames Astrochemistry Laboratory on binary ices containing N_2 mixed with CO, CH_4, O_2, NH_3, H_2O, or CO_2 has demonstrated that the strength of the N≡N stretching fundamental near 2328 cm^{-1} is an extremely strong function of the identity and concentration of other molecules in the ice (Bernstein & Sandford 1999). In this section we briefly review the findings reported in that paper that are of astrophysical relevance.

2.1. *Position and Profile of the Nitrogen Fundamental*

The position and profile of the N≡N stretching fundamental are relatively insensitive to the presence of CO, CH_4, O_2, NH_3, H_2O, and CO_2 over a broad range of concentrations (Bernstein & Sandford 1999). Figure 1 and Table 1 summarize the 2338–2322 cm^{-1} (4.277–4.307 μm) infrared spectra of a pure N_2 ice and six mixed, N_2-rich ices deposited and maintained at 12 K. The spectra were taken at a resolution of 0.9 cm^{-1} (the width of the unresolved line). Pure N_2 produces an absorption band centered at

TABLE 1

POSITIONS, FWHM, AND STRENGTHS OF THE N≡N STRETCHING FEATURES SHOWN IN FIGURE 1

Ice Mixture	Position[a] (cm^{-1})	FWHM (cm^{-1})	*A* Value of N_2[b] (cm molecule^{-1})
"Pure" N_2	2328.2 (4.295)	1.5	$(1.8 \pm 0.3) \times 10^{-22}$[c]
$N_2/CO = 25/1$	2328.2 (4.295)	1.6	$(2.1 \pm 0.7) \times 10^{-22}$
$N_2/CH_4 = 20/1$	2327.9 (4.296)	1.3	$(4.1 \pm 0.7) \times 10^{-22}$
$N_2/O_2 = 20/1$	2328.2 (4.295)	1.4	$(2.4 \pm 0.3) \times 10^{-22}$
$N_2/NH_3 = 22/1$	2328.2 (4.295)	2.0	$(5.1 \pm 0.9) \times 10^{-22}$
$N_2/H_2O = 20/1$	2328.4 (4.295)	3.3	$(1.6 \pm 0.4) \times 10^{-21}$
$N_2/CO_2 = 20/1$	2328.6 (4.294)	1.4	$(1.9 \pm 0.1) \times 10^{-20}$[d]
	2332.0 (4.288)	1.4	

[a] Values in parentheses in the second column are in μm.

[b] *A* values reported in Bernstein & Sandford 1999 using their interference fringe technique.

[c] For comparison, Bohn et al. 1994 report a value of $A_{N2} = (1.3 \pm 0.6) \times 10^{-22}$ cm molecule^{-1}.

[d] Does not include any contribution from the area of the 2332.0 cm^{-1} band.

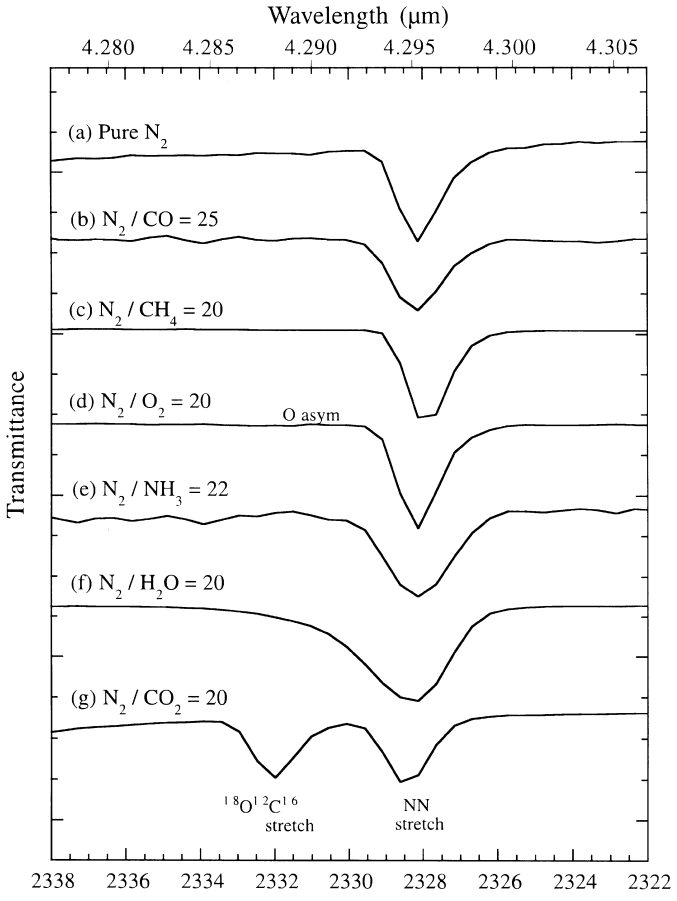

FIG. 1.—2338–2322 cm^{-1} (4.277–4.307 μm) spectra of the N≡N stretching fundamental of (*a*) pure N_2, (*b*) N_2/CO = 25/1, (*c*) N_2/CH_4 = 20/1, (*d*) N_2/O_2 = 20/1, (*e*) N_2/NH_3 = 22/1, (*f*) N_2/H_2O = 20/1, and (*g*) N_2/CO_2 = 20/1 ices deposited and maintained at 12 K. The spectra have all been normalized to show the same band depths.

2328.2 cm^{-1} (4.2952 μm) that has an FWHM of ~1.5 cm^{-1} (0.0028 μm). The addition of 5% CO, CH_4, O_2, or NH_3 has little effect on the position or profile of the N_2 stretching band, although NH_3 does cause the band to broaden slightly. Nitrogen ices containing 5% H_2O produce an N_2 band that is about twice as broad as the other ices. Nitrogen ices containing CO_2 show an N≡N band with a width and position similar to that of the other apolar species plus an additional band at 2332.0 cm^{-1} (4.2882 μm) due to the ^{18}O isotopic band of the CO_2 asymmetric C=O stretching mode.

2.2. *Strength of the Nitrogen Fundamental*

The variability caused in the absorption strength of the N≡N stretch due to molecular environment complicates solid N_2 abundance estimates based on band areas and highlights the need to establish the intrinsic strengths of the N≡N stretch under astrophysically relevant conditions. The relationship between column density (N, in molecules cm^{-2}), intrinsic strength (*A*, in cm $molecule^{-1}$), and peak area ($\int \tau(\nu)d\nu$, in cm^{-1}) is given by

$$A = \frac{\int \tau(\nu)d\nu}{N}.$$

TABLE 2

THE STRENGTH OF THE INFRARED N≡N STRETCHING FEATURE AS A FUNCTION OF GUEST MOLECULE COMPOSITION AND CONCENTRATION

Ice Composition and Ratios	Fraction of Guest Molecule (%)	*A* Value of N_2[a] (cm $molecule^{-1}$)
"Pure" N_2	0.0	$(1.8 \pm 0.3) \times 10^{-22}$[b]
N_2/NH_3:		
22	4.3	$(5.1 \pm 0.9) \times 10^{-22}$
10.4.....	8.8	$(1.6 \pm 0.1) \times 10^{-21}$
4.8	17.2	$(2.6 \pm 0.3) \times 10^{-21}$
0.97.....	50.8	$(8.0 \pm 0.2) \times 10^{-21}$
N_2/H_2O:		
325	0.3	$(2.0 \pm 0.1) \times 10^{-22}$
130	0.8	3.3×10^{-22}[c]
100	1.0	$(4.0 \pm 0.8) \times 10^{-22}$
43	2.3	$(9.5 \pm 1.3) \times 10^{-22}$
20	4.8	$(1.6 \pm 0.4) \times 10^{-21}$
15.5.....	6.1	1.5×10^{-21}[c]
5.0	16.7	3.6×10^{-21}[c]
1.35.....	42.6	$(1.4 \pm 0.1) \times 10^{-20}$
1.0	50.0	$(1.6 \pm 0.1) \times 10^{-20}$
N_2/CO_2:[d]		
400	0.25	$(1.4 \pm 0.1) \times 10^{-21}$
200	0.5	$(4.0 \pm 0.4) \times 10^{-21}$
75	1.3	$(5.3 \pm 0.4) \times 10^{-21}$
20	4.8	$(1.9 \pm 0.1) \times 10^{-20}$
10	9.1	$(4.4 \pm 0.1) \times 10^{-20}$
5.0	16.7	1.2×10^{-19}[c]
3.6	21.7	1.7×10^{-19}[c]
3.0	25.0	$(2.1 \pm 0.1) \times 10^{-19}$
2.25.....	30.8	$(2.7 \pm 0.1) \times 10^{-19}$
2.0	33.3	2.2×10^{-19}[c]

NOTE.—This table is also available in machine-readable form in the electronic edition of the Journal.

[a] *A* values reported in Bernstein & Sandford 1999 using their interference fringe technique.

[b] For comparison, Bohn et al. 1994 report a value of $A_{N2} = (1.3 \pm 0.6) \times 10^{-22}$ cm $molecule^{-1}$.

[c] Result of a single measurement.

[d] *A* values do not include any contribution from the area of the 2332.0 cm^{-1} band.

The presence of CO, CH_4, and O_2 has little effect on the intrinsic strength of the N_2 band (Table 2). Even at large CO, CH_4, and O_2 concentrations, the N_2 band is enhanced in these ices by, at most, a factor of 4. In contrast, the presence of NH_3, H_2O, or CO_2 causes the strength of the N_2 band to increase dramatically as their concentrations rise (Table 2). The effects of these molecules on the strength of the N_2 fundamental are shown graphically in Figure 2. (See Bernstein & Sandford 1999 for a more complete listing of A_{N2} values.)

In N_2-H_2O mixtures, the 2328 cm^{-1} N_2 band strength reaches a value of at least $A_{N2} = 1.4 \times 10^{-20}$ cm $molecule^{-1}$ at $N_2/H_2O = 1$, i.e., almost 80 times greater than for pure solid N_2 ($A_{N2} = 1.8 \times 10^{-22}$ cm $molecule^{-1}$; see Table 2 and Fig. 2). The enhancements produced by NH_3 are less dramatic but still exceed a factor of 40 at high NH_3 concentrations. These band strength enhancements are probably the result of hydrogen-bonding interactions, which are likely also responsible for the band broadening caused by these molecules (Fig. 1). These interactions produce greater breaking of the symmetry of the N≡N stretching vibrations of N_2 in the ice, resulting in greater infrared activation.

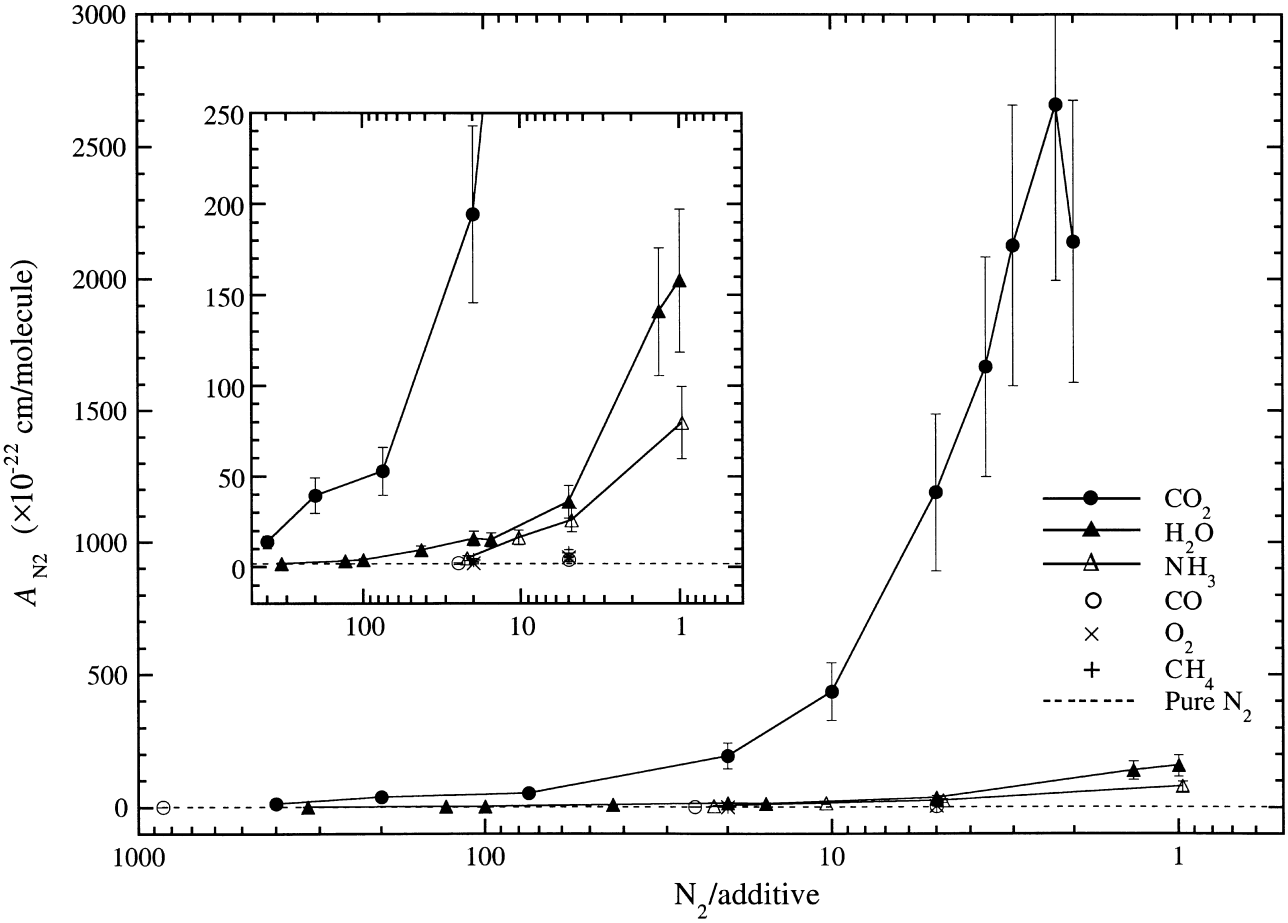

FIG. 2.—Intensity change of the 2328.2 cm^{-1} (4.295 μm) N≡N stretching band as a function of the concentration of added CO_2 (*filled circles*), H_2O (*filled triangles*), NH_3 (*open triangles*), CO (*open circles*), O_2 (*crosses*), and CH_4 (*plus signs*). The values plotted for the N_2-CO_2 ices represent only the contribution from the band near 2328 cm^{-1}, i.e., they do not include the area of the 2332 cm^{-1} $^{18}O^{12}C^{16}O$ band. The dotted horizontal line near the bottom of the figure denotes the absorption strength of the 2328 cm^{-1} N_2 fundamental of a pure nitrogen ice.

The most dramatic effect, however, is produced by CO_2. CO_2 measurably enhances the strength of the N_2 band even at concentrations as low as 0.25%, and at concentrations above 5% it enhances the N_2 band by factors of hundreds. In very CO_2-rich ices the enhancement exceeds a factor of 1000 (Table 2 and Fig. 2). Concentration and isotopic substitution studies show that the enhancement of the N≡N fundamental in N_2-CO_2 ices is due to a resonant interaction of the 2328 cm^{-1} N_2 band with the nearby O=C asymmetric stretches of $^{18}O^{12}C^{16}O$ at 2332 cm^{-1} and $^{16}O^{12}C^{16}O$ at 2348 cm^{-1} (Bernstein & Sandford 1999).

It should be noted that, while it is possible to premix N_2 carefully with other molecules in the gas phase at known concentrations, it is difficult to control the precise extent to which different guest molecules will fractionate relative to the N_2 during deposition. However, this is *not* the cause of the effects just described as the observed enhancements do not correlate in any way with volatility.

Finally, it should be noted that the enhancements produced by NH_3, H_2O, and CO_2 all start to level out as their concentrations exceed about 30%–50% that of the N_2. Calculations suggest that this effect is largely due to nearest neighbor statistics. At guest molecule concentrations above $\sim$30%, nearly every N_2 in the ice sample will be located near a perturbing guest molecule. At this point, the addition of more of the guest molecule will result in little additional perturbation/enhancement of the N_2 fundamental. The observed maxima for NH_3, H_2O, and CO_2 are approximately 8×10^{-21}, 1.5×10^{-20}, and 2.5×10^{19} cm molecule^{-1}, respectively. For more information on the spectral properties of N_2 in mixed molecular ices, see Bernstein & Sandford (1999).

2.3. *The Possible Range of* N_2 *Band Strengths for Interstellar Ices*

The A values in Table 2 and Figure 2 show that the strength of the stretching fundamental of N_2 in ices can vary by orders of magnitude depending on the other molecules in the ice. If the N_2 fundamental is enhanced in interstellar ices, it will be much easier to detect this feature in the infrared spectra of dense molecular clouds. However, it will also be difficult to establish the abundance of any detected N_2 without a complete understanding of the other molecules in the ice. This highlights the need for relevant laboratory spectral data of comparable ice mixtures studied under astrophysically relevant conditions. In the remainder of this section we discuss the range of intensity enhancements that might be expected in interstellar ices and discuss the possible detectability of the 2328 cm^{-1} band of solid interstellar N_2.

Theoretical models predict that the abundance of N_2 relative to CO, CH_4, O_2, NH_3, H_2O, and CO_2 in the ices in

dense molecular clouds should vary considerably depending on the local environmental conditions, H/H_2 ratio, and the clouds' initial elemental composition and age (Tielens & Hagen 1982; d'Hendecourt et al. 1985; Caselli, Hasegawa, & Herbst 1998). However, since lab studies indicate that CO, CH_4, and O_2 produce little or no enhancements in the N_2 fundamental, we can restrict our discussion to the predicted N_2/H_2O, N_2/CO_2, and N_2/NH_3 ice ratios. The range of calculated N_2/H_2O ratios spans values from as low as a few times 10^{-6} to as high as 3, but models restricted to typical conditions and the most relevant timescales generally yield N_2/H_2O ratios of 0.03–0.15. Calculated N_2/CO_2 ratios also cover a wide range, 0.01–1, but again, models restricted to typical conditions and timescales generally yield N_2/CO_2 ratios on the order of 0.4. The calculated N_2/NH_3 ratio appears to be extremely sensitive to environmental conditions, and reported values range from a few times 10^{-3} up to as high as 25. Furthermore, the models do not agree as to what typical N_2/NH_3 values are likely to be, although there is general agreement that the N_2/NH_3 ratios should generally be larger than the N_2/CO_2 ratios.

Examination of Table 2 for these ranges of concentration values indicates that binary mixtures with NH_3 would be expected to produce A_{N2} values from about 8.0×10^{-21} to less than 5.1×10^{-22} cm molecule^{-1} (enhancements of $\sim$45 to $<$3 relative to pure N_2). Binary mixtures with H_2O would be expected to produce values of at least 1.6×10^{-20} cm molecule^{-1} (an enhancement of $\sim$90). More impressively, binary mixtures with CO_2 would be expected to produce enhanced values around 2.5×10^{-19} cm molecule^{-1} (an enhancement of $\sim$1400). Given that all three of these species are seen in interstellar ices, it is likely that the N≡N stretching band of N_2 in interstellar ices is *enhanced by at least a factor of 90, and possibly in excess of a factor of 1000, compared to that of pure* N_2.

Given the likelihood of significant enhancement of the 2328 cm^{-1} N_2 band in interstellar ices, we must ask how difficult it will be to detect it or place significant upper limits on its abundance. The expected optical depth of the N_2 feature (τ_{N2}) can be calculated from $\tau_{N2} \approx (N_{N2} A_{N2})/\Delta\nu_{N2}$, where N_{N2} is the column density of N_2 in molecules cm^{-2}, A_{N2} is the appropriate band strength in cm molecule^{-1}, and $\Delta\nu_{N2}$ is the FWHM of the N_2 band. One can derive the depth of this feature relative to another feature in the spectrum, for example, that of an H_2O ice band, by assuming $N_{N2}/N_{H_2O} = f$, using $N_{H_2O} \approx (\tau_{H_2O} \Delta\nu_{H_2O})/A_{H_2O}$, and substituting into the first equation:

$$\frac{\tau_{N2}}{\tau_{H_2O}} = \frac{f A_{N2} \Delta_{H_2O}}{A_{H_2O} \Delta\nu_{N2}} .$$

In Table 3 we present a series of values for the τ_{N2}/τ_{H_2O} ratio using the 3250 cm^{-1} (3.08 μm) H_2O band and assuming a variety of N_2 band enhancement factors and values of f that span the most likely range, namely, $0.03 < N_{N2}/N_{H_2O} < 0.15$. The band enhancement factors of 1, 30, 90, 350, and 1400 used in Table 3 correspond roughly to the enhancements that would be expected for pure N_2 ice, N_2 in an NH_3-rich ice or an ice containing a few percent H_2O, N_2 in an H_2O-rich ice, N_2 in a mixed N_2:H_2O:CO_2 ice having $N_2/H_2O = 0.03$ and $N_2/CO_2 = 0.4$, and a CO_2-rich ice, respectively. Also, as specific examples, we include in Table 3 the expected optical depth and percent absorption band depth for these various conditions for two specific objects, AFGL 2136 and Elias 16 (see § 3). These values give some indication of the (large) range in N_2 band depths that might be expected in interstellar ices.

It should be noted that the values reported in Table 3 are determined from binary ices. True interstellar ices contain more than two components, however, and this will have some effect on the expected overall enhancement of the N_2 feature. For example, a good spectral fit to the 2140 cm^{-1} feature due to CO in apolar interstellar ices is provided by an ice analog having a composition of N_2:O_2:CO_2:CO = 1:5:0.5:1 (Elsila et al. 1997). Based on Bernstein & Sandford (1999), we could expect the O_2 and CO in this ice to have little effect on the strength of the N≡N stretch, but the CO_2 should have a dramatic effect. This ice has an N_2/CO_2 ratio of 2, for which Table 2 would imply an A_{N2} value of about 2.5×10^{-19} cm molecule^{-1} (an enhancement of a

TABLE 3

EXPECTED STRENGTH OF THE INTERSTELLAR N_2 ICE BAND FOR A VARIETY OF CONDITIONS[a]

N_2 Concentration	Pure N_2[b]	N_2 in NH_3[c]	N_2 in H_2O[d]	N_2 in H_2O:CO_2[e]	N_2 in CO_2[f]
$N_2/H_2O = 0.03$:					
τ_{N2}/τ_{H_2O}[g]	7.4×10^{-6}	1.7×10^{-4}	3.0×10^{-4}	1.3×10^{-3}	1.1×10^{-2}
τ_{N2} in AFGL 2136[h]	2.0×10^{-5} (0.002)	4.6×10^{-4} (0.05)	8.2×10^{-4} (0.08)	3.5×10^{-3} (0.35)	3.0×10^{-2} (3.0)
τ_{N2} in Elias 16[i]	9.3×10^{-6} (0.0009)	2.1×10^{-4} (0.02)	3.8×10^{-4} (0.04)	1.6×10^{-3} (0.16)	1.4×10^{-2} (1.4)
$N_2/H_2O = 0.15$:					
τ_{N2}/τ_{H_2O}[g]	3.7×10^{-5}	8.4×10^{-4}	1.5×10^{-3}	6.5×10^{-3}	5.5×10^{-2}
τ_{N2} in AFGL 2136[h]	1.0×10^{-4} (0.01)	2.3×10^{-3} (0.23)	4.1×10^{-3} (0.41)	1.8×10^{-2} (1.8)	1.5×10^{-1} (13.9)
τ_{N2} in Elias 16[i]	4.7×10^{-5} (0.005)	1.1×10^{-3} (0.11)	1.9×10^{-3} (0.19)	8.2×10^{-3} (0.81)	6.9×10^{-2} (6.7)

[a] The A values and widths used here are those reported in Bernstein & Sandford 1999 using their interference fringe technique. Values of $A_{H_2O} = 1.7 \times 10^{-16}$ cm molecule^{-1} and $\Delta\nu_{H_2O} = 350$ cm^{-1} are used throughout and taken from Hudgins et al. 1993.

[b] Enhancement factor equal to 1. Used $A_{N2} = 1.8 \times 10^{-22}$ cm molecule^{-1} and $\Delta\nu_{N2} = 1.5$ cm^{-1} [for comparison, Bohn et al. 1994 report a value of $A_{N2} = (1.3 \pm 0.6) \times 10^{-22}$ cm molecule^{-1}].

[c] Enhancement factor equal to 30. Used $A_{N2} = 5.4 \times 10^{-21}$ cm molecule^{-1} and $\Delta\nu_{N2} = 2.0$ cm^{-1}.

[d] Enhancement factor equal to 90. Used $A_{N2} = 1.6 \times 10^{-20}$ cm molecule^{-1} and $\Delta\nu_{N2} = 3.3$ cm^{-1}.

[e] Enhancement factor equal to 350. Used $A_{N2} = 6.3 \times 10^{-20}$ cm molecule^{-1} and $\Delta\nu_{N2} = 3.0$ cm^{-1} (H_2O:CO_2:N_2 = 100:7.5:3 ice).

[f] Enhancement factor equal to 1400. Used $A_{N2} = 2.5 \times 10^{-19}$ cm molecule^{-1} and $\Delta\nu_{N2} = 1.4$ cm^{-1}. Values do not include any contribution from the 2332.0 cm^{-1} $^{18}O^{12}C^{16}O$ band.

[g] Ratio of the optical depth of the 2328 cm^{-1} N_2 feature and the 3250 cm^{-1} (3.08 μm) H_2O ice feature.

[h] Used $\tau_{H_2O} = 2.72$ for the 3.08 μm band in AFGL 2136 (Willner et al. 1982). Values in parentheses are in absolute percent.

[i] Used $\tau_{H_2O} = 1.257$ for the 3.08 μm band in Elias 16 (Smith, Sellgren, & Brooke 1993). Values in parentheses are in absolute percent.

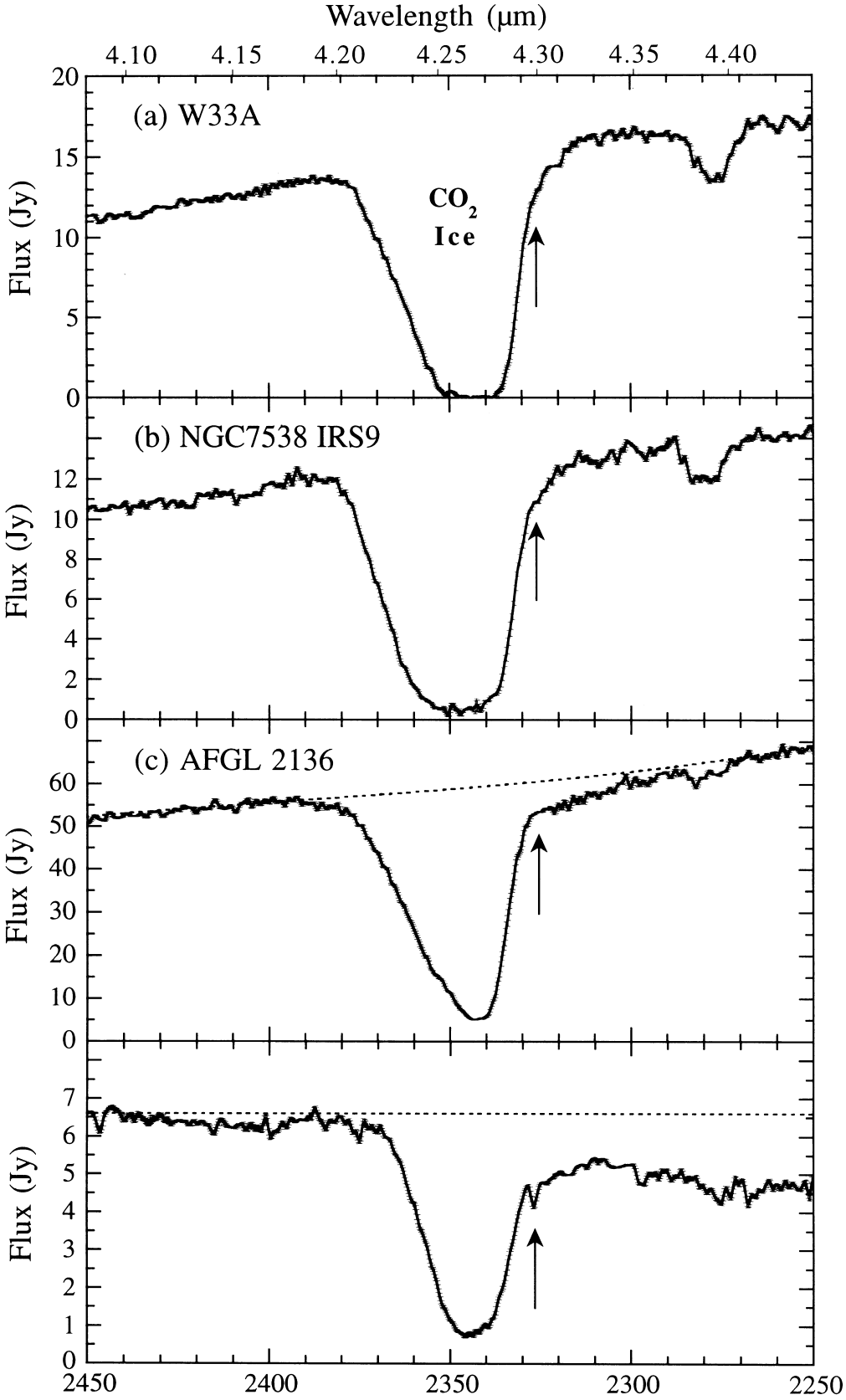

FIG. 3.—2450–2250 cm^{-1} (4.08–4.44 μm) spectra of several infrared sources along lines of sight passing through dense molecular cloud material: protostars (*a*) W33A, (*b*) NGC 7538 IRS 9, (*c*) AFGL 2136, and (*d*) a background field star, Elias 16. The strong band centered near 2345 cm^{-1} (4.26 μm) is due primarily to CO_2 frozen in interstellar ices. The isotopic band due to $^{13}CO_2$ in the ices is also visible in the spectra near 2280 cm^{-1} (4.39 μm). The expected position of the N_2 fundamental is marked with a vertical arrow in each spectrum. The dotted lines superimposed on the spectra of AFGL 2136 and Elias 16 represent the baselines used to calculate the optical depths shown in Figs. 4 and 7.

factor of ~ 1400 over a pure N_2 ice). However, the actual N_2 band strength enhancement in this ice is mitigated by the other, nonenhancing molecules in the ice. Molecules like O_2, CO, and CH_4 may not effect the N_2 fundamental themselves, but they will partially isolate the N_2 from the other molecules that do, thereby decreasing the total enhancement. This increased isolation will be most important in environments with the lowest H/H_2, i.e., the environments where very nonpolar ices dominate. However, even under these conditions a significant fraction of the N_2 molecules within the ice will still have an NH_3, H_2O, or CO_2 neighbor. For example, in the case of an $N_2:O_2:CO_2:CO = 1:5:0.5:1$ ice, where the O_2 and CO provide significant isolation of the N_2, we still expect $\sim 70\%$ of the N_2 to have at least one CO_2 neighbor. Thus, one would expect this ice to produce an N_2 feature with an A_{N2} value in the neighborhood of 1.8×10^{-19} cm molecule^{-1} (enhancement factor of ≈ 1000). This is consistent with the value of $\sim 2 \times 10^{-19}$ cm molecule^{-1} (enhancement of ~ 1100) that we actually observe for an $N_2:O_2:CO_2:CO = 1:5:0.5:1$ ice.

Thus, laboratory studies demonstrate that the strength of the N_2 band produced by interstellar ices should be substantially enhanced relative to that of a pure N_2 ice. Such enhancements should significantly improve the possibility of direct detection of N_2 in interstellar ices but will complicate the interpretation of any N_2 bands thereby detected.

3. ASTRONOMICAL SPECTRA

To search for the absorption band of N_2 ice in interstellar dense clouds, one must measure the spectrum of a "background" infrared source. The source can either be a star that lies behind the dense cloud or a protostar embedded within. In the former case the line of sight will be dominated by the general, quiescent cloud medium, while in the latter case it will include contributions from material in both the general cloud and the "local" concentration of material associated with the forming star. The abundance of N_2-containing ices along these two types of lines of sight may be very different, both because they represent environments having different H/H_2 ratios, chemical evolutionary histories, etc., and because the dust associated with embedded protostars is considerably warmer than in the general cloud medium. Volatile N_2 is more likely to have been lost from the grains via sublimation in the vicinity of protostars than in the general cloud medium. This would be in keeping with observations that these two types of lines of sight show different distributions in other ice-related materials (see Sandford et al. 1988; Tielens et al. 1991; Tegler et al. 1995; Whittet et al. 1996; Gerakines et al. 1999). Thus, ideally, a search for interstellar N_2 would include the use of both types of objects as background sources. To this end, we now consider the spectra of four infrared sources, three protostars and a star located behind a dense cloud.

The astronomical spectra described here were obtained with the *ISO* short-wavelength spectrometer (SWS; de Graauw et al. 1996a), used in grating mode AOT06. The spectra of the protostellar sources, W33A, NGC 7538 IRS 9, and AFGL 2136, are from Teixeira et al. (1999). Details on how those data were obtained and reduced are given in that paper. (Note that in Teixeira et al. 1999 the coordinates of NGC 7538 IRS 9 and AFGL 2136 were accidentally switched: the former object is located at $\alpha_{2000} = 23^h14^m01^s$, $\delta_{2000} = 61°27'20''$, while the latter is located at $\alpha_{2000} = 18^h22^m26^s$, $\delta_{2000} = -13°30'08''$.) The raw data of Elias 16 ($\alpha_{2000} = 04^h39^m38^s$, $\delta_{2000} = 26°11'25''$), a K1 III field star behind the Taurus molecular cloud (Elias 1978), were retrieved from the *ISO* Data Archive, from an original proposal by D. C. B. Whittet.

Data reduction of the protostellar objects was carried out in 1998 August using the *ISO* SWS IA[3] package and the calibration files available at the time. Reduction of the Elias 16 data was done with OSIA v1.0. In all cases, data processing departed from the pipeline at the standard processed data stage. Dark revision and subtraction, as well as correction of glitches, jumps, and differences between up and down scans, were performed interactively. After extracting the spectra with filtering to the instrumental resolution for point sources for the relevant band(s) (1E and 2A in the case of the protostellar objects and 2A in the case of Elias 16), the spectra were further Hanning-smoothed using ISAP. The width of the smoothing bin was 0.0020375 μm for the protostellar objects and 0.002135 μm for Elias 16.

Figure 3 shows the resulting 2450–2250 cm^{-1} (4.08–4.44 μm) spectra of W33A, NGC 7538 IRS 9, AFGL 2136, and Elias 16. The first three of these infrared sources are protostars that probe a line of sight that passes through both quiescent dense molecular cloud material and material more local to the protostar. Elias 16 is a K1 III background star behind a dense cloud and is expected to probe only quiescent dense molecular cloud material. The expected position of the N_2 fundamental is marked with a vertical arrow in each spectrum. The dotted lines superimposed on the spectra of AFGL 2136 and Elias 16 (Figs. 3*c* and 3*d*) represent the baselines used to calculate the optical depths of the absorption bands seen in this spectral region (see §§ 4.1 and 4.2).

A band near 2345 cm^{-1} (4.26 μm) due to solid-state CO_2 dominates all the spectra. This band is badly saturated in the spectra of W33A and NGC 7538 IRS 9 and is becoming saturated in the spectra of AFGL 2136 and Elias 16. A second, weaker feature seen near 2280 cm^{-1} (4.39 μm) is due to solid-state $^{13}CO_2$. For more detailed descriptions of the interpretation of these features, the reader is invited to see Gerakines et al. (1999). While not visible on the scale of these figures, several of the spectra show evidence for the presence of the rotation lines of gas-phase CO_2 (see van Dishoeck et al. 1996 and § 4.1).

4. UPPER LIMITS ON N_2 ICE COLUMN DENSITIES

The detection of the interstellar 2328 cm^{-1} (4.295 μm) feature of solid N_2 is fraught with difficulty that extends beyond the problems associated with the intrinsic weakness of the band and its strong variability as a function of ice composition. Three added complications, at least for the astronomical data currently available, are (1) the presence of the strong, nearby $^{12}CO_2$ ice feature that complicates the selection of the baseline of any N_2 feature present; (2) the presence, especially for the lines of sight toward protostars, of gas-phase CO_2 that produces a system of molecular rotation lines that straddle the N_2 band position; and (3) in the case of the background star Elias 16, the presence of absorption lines in the same spectral region due to photospheric CO. As a result, we can currently only derive upper limits to the amounts of N_2 present toward these objects. In the sections that follow we examine the lines of sight toward protostars (particularly AFGL 2136; § 4.1) and the background field star Elias 16 (§ 4.2) and then briefly discuss

some implications of our work for the detection of N_2 in solar system objects (§ 5).

4.1. *Upper Limits on the Amount of* N_2 *in Interstellar Ices on the Line of Sight toward Protostars*

It is apparent from Figure 3 that it is very difficult to address the abundance of solid N_2 toward W33A and NGC 7538 IRS 9 because the N_2 band position falls on the slope of the extremely strong, saturated 2345 cm^{-1} CO_2 ice bands in their spectra. These spectra serve to demonstrate the enormous difficulty involved with detecting N_2 ice along lines of sight with very large column densities. In the discussion that follows we will concentrate on the spectrum of AFGL 2136, which has considerably less CO_2 ice band saturation. A continuum fit to the spectrum of AFGL 2136 was made using the same procedure as that of Gerakines et al. (1999), i.e., a third-order polynomial was fitted to the data points in the 4.0–4.1 and 4.4–4.5 μm spectral intervals. This baseline is shown as a dotted line in Figure 3*c* and was used to generate the optical depth plot shown in Figure 4.

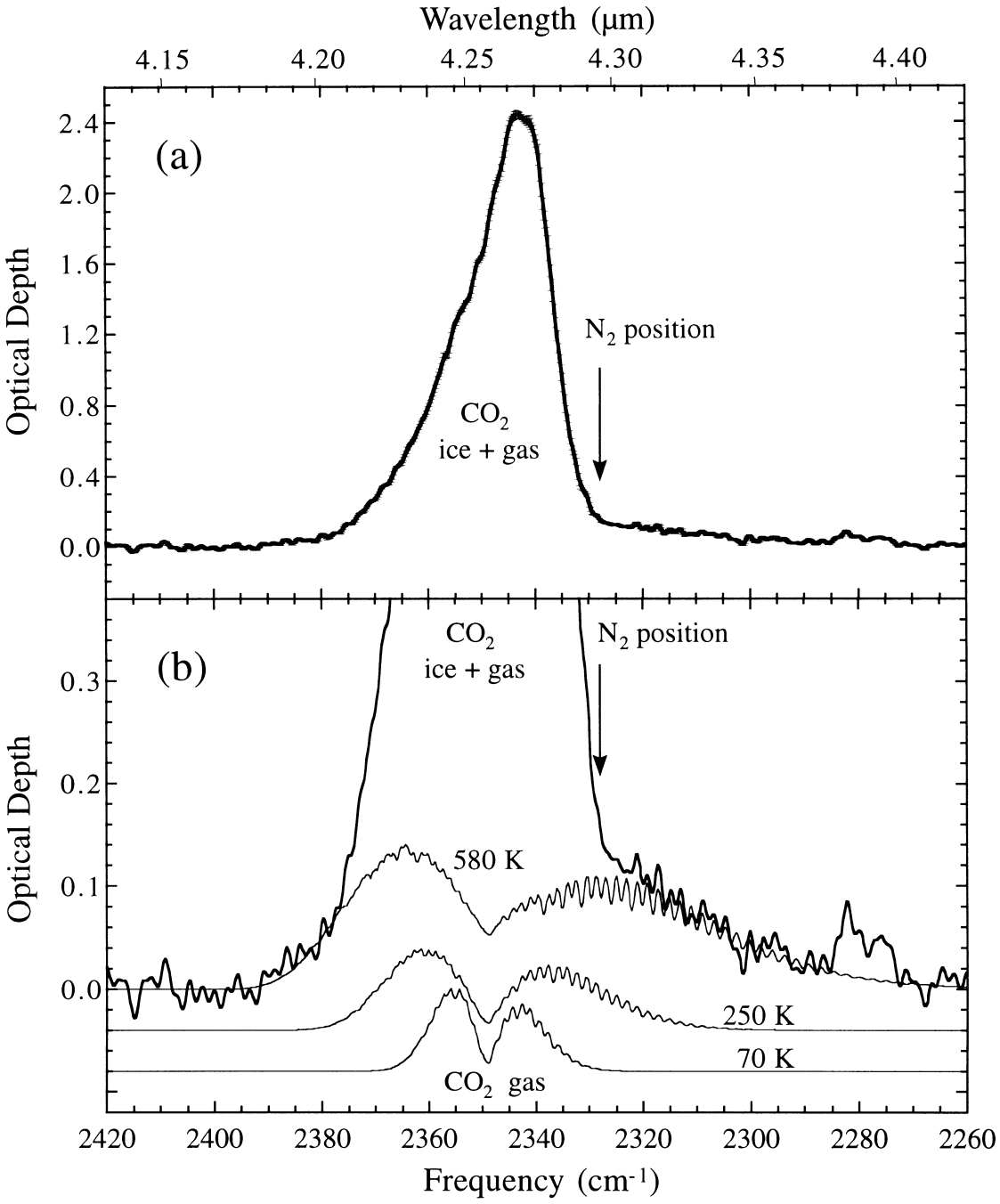

FIG. 4.—2420–2260 cm^{-1} (4.13–4.42 μm) optical depth plot of (*a*) the CO_2 ice feature toward AFGL 2136 derived from the data and baseline shown in Fig. 3*c* and (*b*) the base of the AFGL 2136 CO_2 ice feature compared to the contributions expected from gas-phase CO_2 at 70, 250, and 580 K (see § 4.1). The 70 and 250 K CO_2 gas spectra in (*b*) have been displaced downward for clarity. The vertical arrows indicate the expected position of the solid-state N_2 feature.

As a very conservative upper limit on the column density of N_2 toward this object, one could simply use the optical depth at the 2328 cm^{-1} N_2 band position in the spectrum in Figure 4. However, it is known that this line of sight contains gas-phase CO_2 (van Dishoeck et al. 1996; Gerakines et al. 1999), the rotational lines of which can produce substantial absorption across the N_2 band position. We have examined the consequences of compensating for the gas-phase CO_2 contribution using a technique similar to that used by Gerakines et al. (1999).

The HITRAN 96 database was used to calculate the expected CO_2 lines for gases having temperatures of 70, 250, and 580 K using the HAWKS software (Rothman et al. 1998). Calculations were made for both the CO_2 asymmetric stretching mode lines in the 2430–2240 cm^{-1} (4.12–4.46 μm) region and the O=C=O bending mode lines in the 720–610 cm^{-1} (13.9–16.4 μm) region. Only the $^{12}C^{16}O_2$ lines were calculated. The bands were then convolved with a Gaussian function with a fixed FWHM designed to match the resolution of the synthetic CO_2 spectra with the smoothed astronomical data. The FWHM used was 1.55 cm^{-1} for the CO_2 stretching band and 0.445 cm^{-1} for the CO_2 bending band.

Each of the 70, 250, and 580 K synthetic bending mode spectra were then scaled so that the central, unresolved Q-branch of the CO_2 ν_2 band at 668 cm^{-1} (14.97 μm) matched the depth of the same feature in the data of AFGL 2136 from Gerakines et al. (1999). Figure 5 shows an example of this matching for the case of a 580 K CO_2 gas. The resulting scaling factors were then used to scale the strengths of the synthetic CO_2 ν_3 asymmetric stretching mode rotation lines. Figure 4*b* shows the CO_2 gas-phase absorption contributions that would be expected in the 2420–2260 cm^{-1} region if these different temperature gases were responsible for the 668 cm^{-1} CO_2 Q-branch (the 70 and 250 K spectra have been offset downward for clarity). Each of these contributions could then be subtracted from the overall optical depth spectrum of AFGL 2136.

The best fit to the data, both in absolute strength and overall profile, is provided by the 580 K gas. The presence of warm CO_2 gas is not entirely unexpected since this temperature is nearly the same as the blackbody temperature inferred from the infrared continuum emitted by the dust shell surrounding this protostar (Willner et al. 1982), and 580 K CO gas has been measured along this line of sight (Mitchell et al. 1990). This suggests that the observed CO_2 gas may be largely associated with the protostar, presumably in a zone where its radiation is causing the sublimation of nearby interstellar ices. It should be pointed out, however, that the good fit produced by the 580 K CO_2 gas

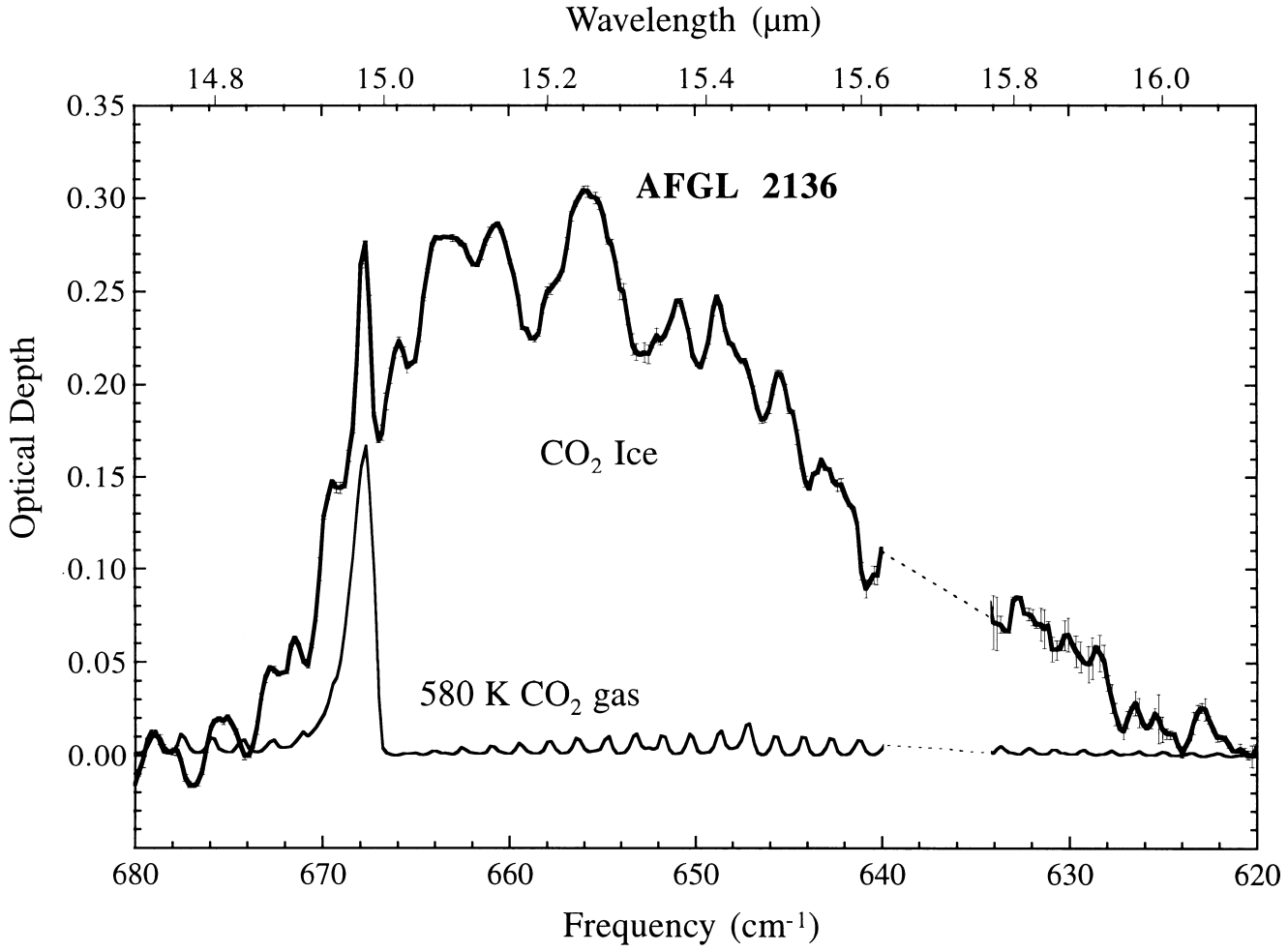

FIG. 5.—680–620 cm^{-1} (14.7–16.1 μm) optical depth plot of AFGL 2136 (from Gerakines et al. 1999) compared to the scaled synthetic spectrum of a 580 K CO_2 gas calculated using HITRAN (see § 4.1). The strong feature at 668 cm^{-1} is due to the unresolved Q-branch rotation lines of the bending mode vibrations of gas-phase CO_2. The broader absorption is due to solid-state CO_2, and its position and profile provide extensive information about the state and composition of the ice (Ehrenfreund et al. 1998b; Gerakines et al. 1999).

does not preclude the presence of some CO_2 gas at lower temperatures, as such contributions would fall more under the solid CO_2 ice feature where it is not possible to constrain their presence by fitting to the data (see Fig. 4*b*). However, only a small amount of cold gas could be added in this manner without violating the initial constraint provided by the strength of the 668 cm^{-1} CO_2 Q-branch. In any event, the presence of colder CO_2 gases is less critical to the issue at hand since they would contribute significantly less absorption to the N_2 band position.

Figure 6 shows the residual AFGL 2136 CO_2 ice feature remaining after the contributions of CO_2 gas at temperatures of 70, 250, and 580 K have been removed. While all these spectra show a minor absorption "bump" at the 2328 cm^{-1} N_2 band position, it is not larger than many other deviations in the spectrum, i.e., none of these spectra show compelling evidence for the presence of a distinct band at the N_2 ice band position. The total residual optical depths at the 2328 cm^{-1} N_2 ice band position in Figure 6 could be used to derive a very conservative estimate of the absorption due to solid N_2 along this line of sight (i.e., $\tau \approx 0.18$, 0.13, and 0.07 for the 70, 250, and 580 K CO_2 gas subtractions, respectively). However, assuming that all the absorption at this position is due to N_2 would result in the remaining absorption having a very peculiar profile, especially for the spectra with lower temperature gas-phase CO_2 removed. For example, if all the absorption at 2328 cm^{-1} in the spectrum in Figure 6*a* was due to solid N_2, the remaining absorption profile would have to drop from $\tau \sim 0.20$ at 2330 cm^{-1} to zero absorbance at around 2329 cm^{-1} and then spring back up to about $\tau \sim 0.13$ at about 2327 cm^{-1} before continuing its monotonic descent to zero near 2290 cm^{-1}. Such a profile is clearly highly unlikely. A more reasonable estimate of the maximum absorption that could be due to solid N_2 can be found by determining, in each case, the maximum amount of absorption that can be removed from the 2–3 cm^{-1} wide region centered on the N_2 band position without causing a significant discontinuity in the profile of the wing of the CO_2 ice feature. In all three cases, this corresponds to upper limits on the N_2 absorption that are largely defined by the signal-to-noise ratio (S/N) of the data in this region, i.e., a conservative value of $\tau \sim 0.04$ in all three cases. Table 4 shows the limiting N_2 column densities and the N_2/H_2O and N_2/CO_2 ratios to which this value corresponds for the various enhancement factors described in § 2 and summarized in Table 3. The implications of these upper limits are discussed in § 5.

4.2. *Upper Limits on the Amount of* N_2 *in Interstellar Ices on the Line of Sight toward Elias 16*

Figure 7*a* shows the optical depth plot of Elias 16 derived from the spectrum and baseline shown in Figure 3*d* (see below for how the baseline was determined). Since Elias 16 is a background star behind the Taurus dense cloud, this line of sight should not be associated with any of the locally heated dust seen toward the protostars. Instead, it should be dominated by material in the quiescent cloud medium where temperatures are expected to be very low. Thus, gas-phase CO_2 should not represent as significant a problem as it did for the analysis of the AFGL 2136 spectrum. In addition, based on theoretical considerations, quiescent parts of interstellar clouds are expected to contain a larger proportion of N_2-bearing apolar ices.

Unfortunately, the spectrum of Elias 16 suffers from a different problem. Elias 16 is a cool K1 III field star whose spectrum contains substantial absorption from photospheric CO. While the center of the *R*- and *P*-branches of the stretching mode rotation lines of gas-phase CO falls near 2140 cm^{-1} (4.67 μm), the photospheric temperature of Elias 16 is sufficiently high (4580 K) that *R*-branch lines of highly excited states of the CO extend into the region of interest for the N_2 feature. Indeed, one of the CO band heads falls almost directly on top of the N_2 band position.

In order to account for this absorption contribution, we again calculated a synthetic gas-phase spectrum. We used the $^{12}C^{16}O$ lines between 2400 and 2200 cm^{-1} from the line list of Goorvitch (1994). The strength of these lines was calculated for a temperature of 4580 K using the partition function, term energies, and transition frequencies given by Goorvitch (1994) and the well-known formula for the ratio of line strengths at two different temperatures. The bands were then convolved with a Gaussian function with a fixed FWHM that matched the resolution of the synthetic spectrum with the smoothed astronomical data (FWHM = 1.55 cm^{-1}). Figure 7*a* shows the optical depth spectrum of Elias 16 compared to the convolved spectrum expected from a

TABLE 4

UPPER LIMITS ON THE N_2 COLUMN DENSITY AND N_2/H_2O AND N_2/CO_2 RATIOS IN AFGL 2136 AND ELIAS 16[a]

N_2 Concentration	Pure N_2[b]	N_2 in NH_3[c]	N_2 in H_2O[d]	N_2 in H_2O:CO_2[e]	N_2 in CO_2[f]
AFGL 2136 ($\tau_{N2} \leq 0.04$):					
Maximum N_{N2}[g]	$<3.3 \times 10^{20}$	$<1.5 \times 10^{19}$	$<8.3 \times 10^{18}$	$<1.9 \times 10^{18}$	$<2.2 \times 10^{17}$
Maximum N_2/H_2O	<65	<2.9	<1.6	<0.4	<0.04
Maximum N_2/CO_2[h]	<540	<25	<14	<3.1	<0.4
Elias 16 ($\tau_{N2} \leq 0.08$):					
Maximum N_{N2}[g]	$<6.7 \times 10^{20}$	$<3.0 \times 10^{19}$	$<1.7 \times 10^{19}$	$<3.8 \times 10^{18}$	$<4.5 \times 10^{17}$
Maximum N_2/H_2O	<260	<12	<6.4	<1.5	<0.2
Maximum N_2/CO_2[h]	<1460	<65	<37	<8.3	<1.0

[a] The values presented in this table were all derived using the same parameters used in Table 3.
[b] Enhancement factor equal to 1.
[c] Enhancement factor equal to 30.
[d] Enhancement factor equal to 90.
[e] Enhancement factor equal to 350.
[f] Enhancement factor equal to 1400.
[g] Units are in molecules cm^{-2}.
[h] Calculated using $N_{CO_2} = 6.1 \times 10^{17}$ cm^{-2} for AFGL 2136 (de Graauw et al. 1996b) and $N_{CO_2} = 4.6 \times 10^{17}$ cm^{-2} for Elias 16 (Whittet et al. 1998).

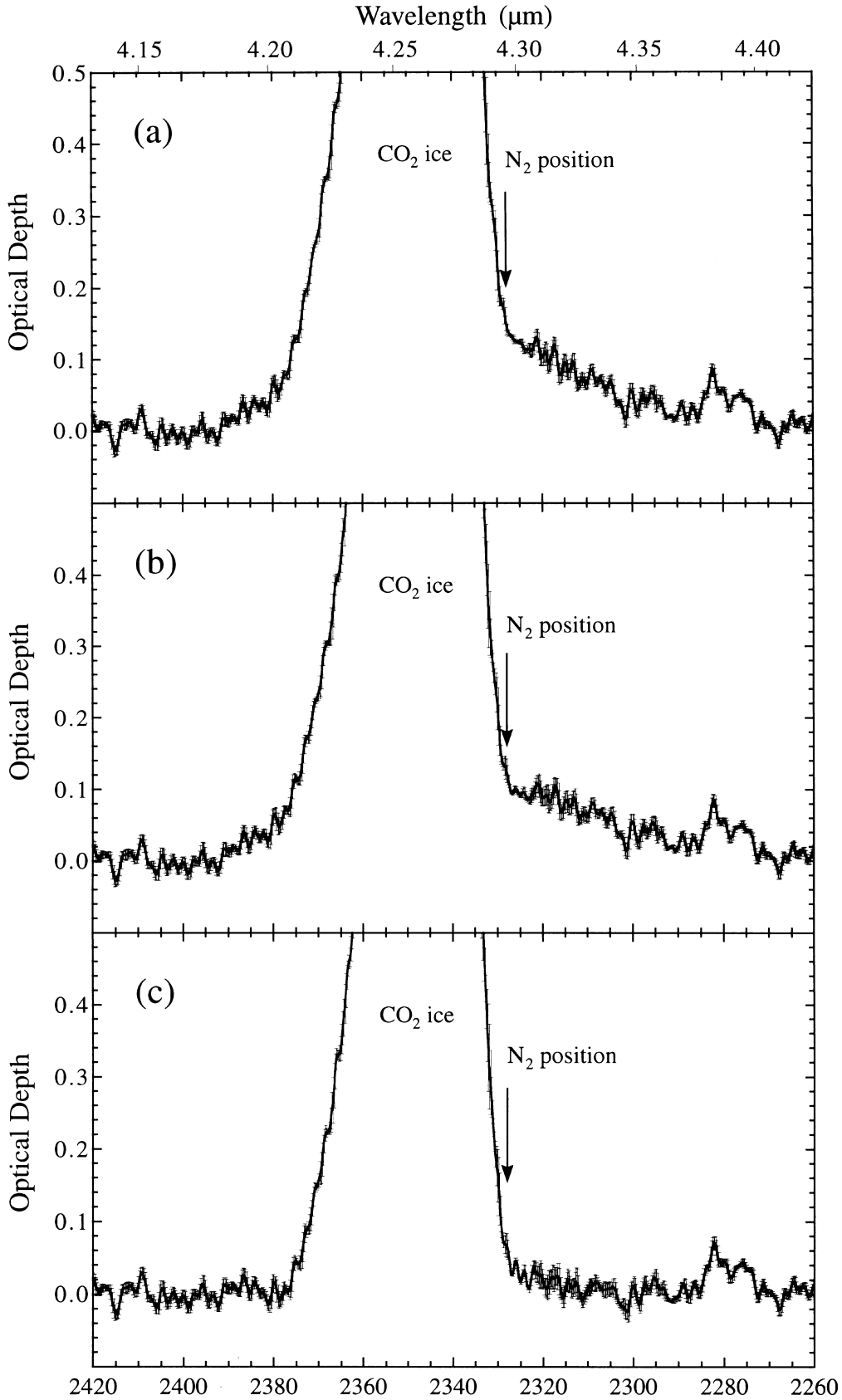

FIG. 6.—Residual AFGL 2136 CO_2 ice feature that remains after contributions of CO_2 gas at temperatures of (*a*) 70 , (*b*) 250, and (*c*) 580 K have been removed in a manner consistent with the observed strength of the unresolved *Q*-branch rotation lines at 668 cm^{-1}. The vertical arrows indicate the expected position of the solid-state N_2 feature.

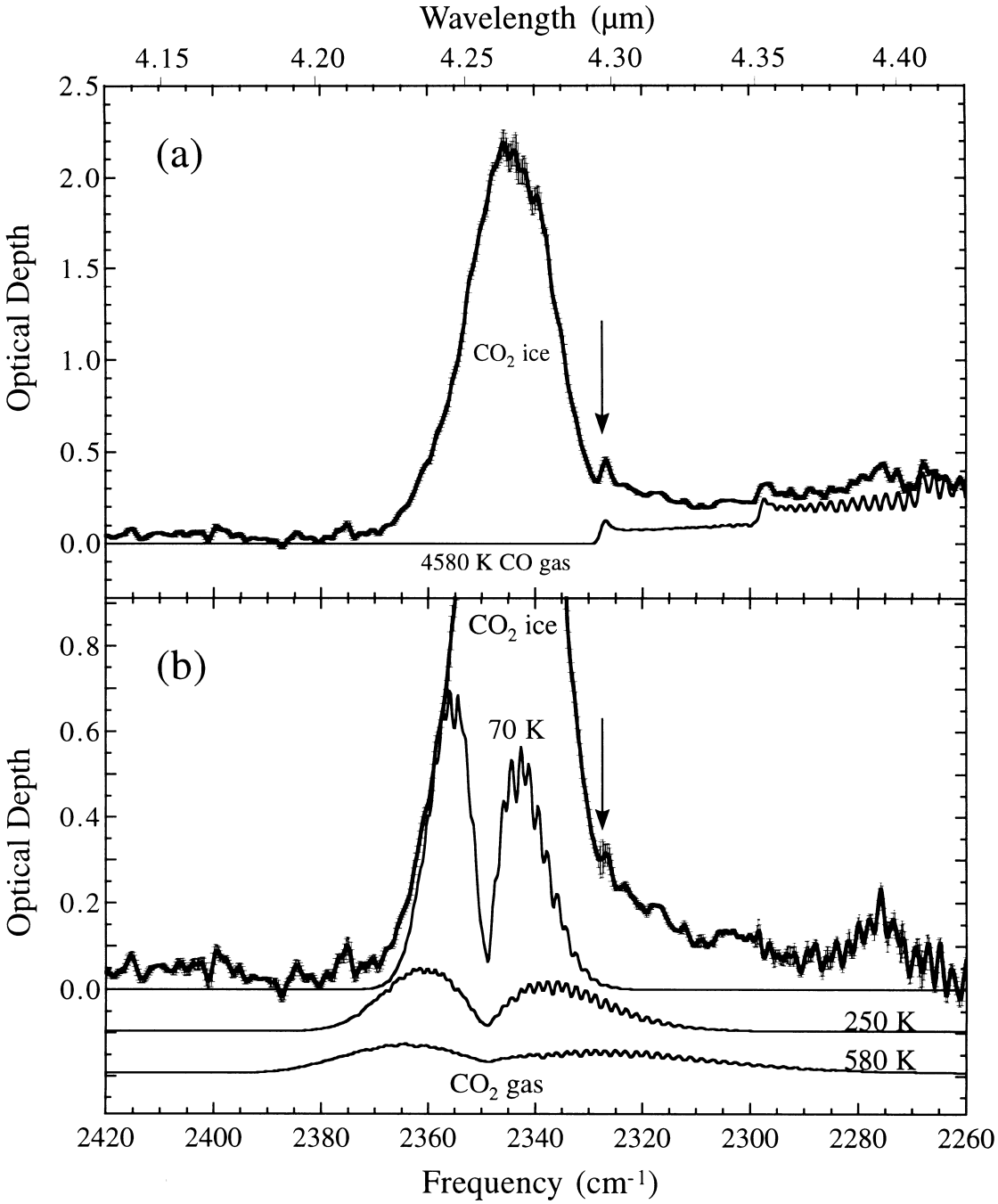

FIG. 7.—2420–2260 cm^{-1} (4.13–4.42 μm) optical depth plot of (*a*) the CO_2 ice feature toward Elias 16 derived from the data and baseline shown in Fig. 3*d*, compared with the synthetic spectrum of a 4580 K CO gas; and (*b*) the base of the Elias 16 CO_2 ice feature after removal of photospheric CO compared to the maximum possible contributions that could be made by gas-phase CO_2 at 70, 250, and 580 K (see § 4.2). The 250 and 580 K CO_2 gas spectra in (*b*) have been displaced downward for clarity. The vertical arrows indicate the expected position of the solid-state N_2 feature.

4580 K CO gas. Note the local peaks near 2327, 2298, and 2269 cm^{-1} due to the *R*-branch $0 \rightarrow 1$, $1 \rightarrow 2$, and $2 \rightarrow 3$ transition band heads, respectively, which are apparent in both the synthetic spectrum and that of Elias 16. The $0 \rightarrow 1$ band head falls almost directly on the N_2 ice position.

Since the photospheric CO absorption extends all the way to the edge of the CO_2 ice feature, it is not possible to establish a baseline across this spectral region by simply fitting a line or polynomial to the data as was done for AFGL 2136. Instead, it was necessary to carry out a simple iterative process in which a baseline was selected, an optical depth plot derived, the photospheric CO contribution removed, and the resulting absorption spectrum investigated for evidence of residual photospheric CO *R*-branch $0 \rightarrow 1$, $1 \rightarrow 2$, and $2 \rightarrow 3$ band head features. Residual CO features were then used to iterate the chosen baseline until the solution converged on a baseline that yielded negligible CO features in the final spectrum. This resulted in the baseline shown in Figure 3*d* that was used to derive the optical depth plot shown in Figure 7*a*. Figure 7*b* shows the residual spectrum resulting from the removal of the synthetic photospheric CO contribution. Note that a very weak feature remains at the position of the N_2 ice band position, but its strength is comparable to the CO rotational line residuals

seen in the spectrum in the 2290–2260 cm^{-1} region and is most likely the result of a small amount of uncorrected photospheric CO.

Dealing with the issue of possible contributions from gas-phase CO_2 along the line of sight is problematic since no useful data are available in the 700–600 cm^{-1} spectral region for this object. Thus, it is not possible to use the strength of a 668 cm^{-1} CO_2 gas-phase Q-branch to constrain the possible abundance of CO_2 gas, as was done for AFGL 2136. Figure 7*b* shows the profiles and intensities of the *maximum* possible contributions from gas-phase CO_2 at temperatures of 70, 250, and 580 K that are compatible with the residual spectrum. In all cases, the strongest constraint is supplied by requirement that the CO_2 contribution not exceed the observed absorption in the 2375–2355 cm^{-1} range (see Fig. 7*b*). Because of its narrower rotational envelope, considerable absorption from cold CO_2 gas can be accommodated by the data. However, CO_2 gas at temperatures of 70 K produces very little absorption at 2328 cm^{-1} and therefore is of little consequence to deriving the upper limit on N_2 abundance. At most, 70 K CO_2 gas could be responsible for only about 6% of the absorption at this position (≤ 0.02 out of a total τ of 0.33). Little warm gas (250 and 580 K) would be expected in the quiescent dense cloud medium, which is consistent with the observation that very little can be introduced without exceeding the observed absorption at the high-frequency wing of the CO_2 ice feature. As a result, the maximum possible contribution of warm CO_2 gas at the 2328 cm^{-1} N_2 ice band position is small ($\tau < 0.07$ or less than 20% of the absorption at this position for a 250 K gas and $\tau \leq 0.05$ or less than 15% for a 580 K gas). (We would note that a cold CO_2 gas abundance as high as the maximum shown in Fig. 7*b* is highly unlikely since (1) CO_2 should begin to freeze efficiently onto grains at these temperatures and (2) it would require that the observed, roughly Gaussian CO_2 profile shown in Fig. 7*a* be made from the superposition of a double-lobed CO_2 gas-phase spectrum and a fortuitously offset double-lobed CO_2 ice feature unlike that seen in the spectra of any reasonable laboratory astrophysical analog ices so far examined; Sandford & Allamandola 1990; Gerakines et al. 1999.)

As with AFGL 2136, the total residual optical depths at the 2328 cm^{-1} N_2 ice band position could be used to derive a very conservative estimate of the absorption due to solid N_2 along this line of sight, but this would result in the remaining absorption having a very peculiar profile. Again, a more reasonable estimate of the maximum absorption that could be due to solid N_2 can be found by determining the maximum amount of absorption that can be removed from the 2–3 cm^{-1} wide region centered on the N_2 band position without causing a significant discontinuity in the profile of the wing of the CO_2 feature. Independent of any underlying minor contribution from gas-phase CO_2, this corresponds to upper limits on the N_2 absorption that are largely defined by the quality of the residual data in this region, which, unfortunately, have both a lower S/N than the AFGL 2136 data and additional uncertainty associated with the possible presence of a small residual of the R-branch $0 \rightarrow 1$ photospheric CO band head. A conservative upper limit for the maximum absorption at 2328 cm^{-1} due to solid N_2 in the spectrum of Elias 16 is $\tau \sim 0.08$, i.e., about twice the upper limit found for AFGL 2136 . Table 4 shows the limiting N_2 column densities and the N_2/H_2O and N_2/CO_2 ratios to which this value corresponds for the various enhancement factors described in § 2 and summarized in Table 3. The implications of these upper limits are discussed in § 5.

5. DISCUSSION AND ASTROPHYSICAL IMPLICATIONS

5.1. *Constraints on the Abundance and Composition of N_2-bearing Interstellar Ices*

While no clear detection of N_2-bearing ices resulted from the efforts described above, examination of Tables 3 and 4 demonstrates that the N_2 column density upper limits derived from AFGL 2136 and Elias 16 are sufficiently low to begin to eliminate some possibilities.

As mentioned earlier, the range of theoretically predicted N_2/H_2O ratios ranges from a few times 10^{-6} to as high as 3, but typical environments are generally expected to have N_2/H_2O ratios of 0.03–0.15. The N_2/H_2O upper limits given in Table 4 are already sufficient to eliminate the higher theoretical values, at least for ices in which the N_2 band strength is enhanced by the presence of CO_2 and, in the case of AFGL 2136, by H_2O. Even the nominal predicted N_2/H_2O values of 0.03–0.15 are precluded in AFGL 2136 if there is band enhancement by CO_2 (although note that lower N_2/H_2O ratios than predicted might well be expected for this object since local heating is likely to cause the evaporation of some or all of the local N_2). None of the current upper limits preclude the theoretical range of N_2 relative to H_2O in "typical" environments for ices in which the N_2 band is either unenhanced or enhanced only by the presence of NH_3 or H_2O.

A similar analysis can be made for N_2/CO_2 ratios. Calculated N_2/CO_2 ratios also span a wide range, 0.01–1, but models restricted to more typical conditions and timescales generally yield predicted N_2/CO_2 ratios on the order of 0.4. The upper limits derived in this work are just beginning to approach the higher theoretical values, at least for ices in which CO_2 is causing maximal enhancement of the N_2 band strength. Truly meaningful tests of theoretical N_2/CO_2 ratios will have to await improved upper limits or actual detection of the interstellar N_2 feature.

5.2. *Gas-Phase CO_2 around AFGL 2136 and the Apolar Ice Component*

The fit to, and removal of, a 580 K CO_2 gas in the spectrum of AFGL 2136 has several implications. Gas-phase CO_2 was first identified along the line of sight to this object by van Dishoeck et al. (1996) through the detection of the unresolved Q-branch of the CO_2 ν_2 band at 668 cm^{-1} (14.97 μm), which provides no information about the CO_2 gas temperature. Based on HITRAN calculations for 25 and 250 K CO_2 gases, they tentatively derived a gas-phase CO_2 column density of 1×10^{16} cm^{-2} from the detected ν_2 band. On the basis of a lack of obvious ν_3 P- and R-branch structure superimposed on the CO_2 ice feature near 2345 cm^{-1}, they derived an independent CO_2 upper limit of $N_{CO_2} < 5 \times 10^{16}$ cm^{-2}.

As the assumed temperature of the CO_2 gas is increased, the abundance of the gas-phase CO_2 inferred from the ν_2 Q-branch will also increase. For our 70, 250, and 580 K fits to ν_2 Q-branch we derive CO_2 gas column densities of 1.9×10^{16}, 3.1×10^{16}, and 8.4×10^{17} cm^{-2}, respectively. Thus, if the CO_2 gas is, in fact, cool ($T \leq 250$ K), we find gas-phase CO_2 column densities that are reasonably consistent with those of van Dishoeck et al. (1996), albeit a bit larger. However, if the CO_2 gas is warmer (580 K), we find

that there could be almost an order of magnitude more CO_2 in the gas phase than tentatively derived by van Dishoeck et al. (1996) on the basis of lower assumed gas temperatures. Although this sounds like a large difference, it does not in any way alter their major conclusion, namely, that the majority of CO_2 along this line of sight is in the solid form. It would, however, correspond to a gas/solid CO_2 ratio along this line of sight of ~ 0.17, rather than the value of 0.02 they report. One of the puzzles raised by their earlier work was how the gas/solid ratio could be so low for CO_2 (0.02) while being significantly higher for both lower volatility H_2O (0.4) and higher volatility CO (200). The presence of warm CO_2 gas mitigates the need for the overall reservoir of CO_2 to have quite such a peculiar behavior.

The presence of warmer CO_2 gas may also have some implications for the interpretation of the 2345 cm^{-1} CO_2 ice feature. Gerakines et al. (1999) used data from a variety of laboratory ice analogs to interpret the profile of the CO_2 ice feature in the spectrum of AFGL 2136. Prior to attempting to fit the ice feature, they removed a gas-phase contribution from this feature in the same manner we described in § 4.1. However, they removed a gas-phase contribution with an assumed temperature of only 250 K. The presence of warmer gas has several effects: it increases the total ν_3 absorption relative to ν_2 absorption, and it increases the spectral range over which the ν_3 rotational envelope extends. Thus, subtraction of a warmer gas results in residual CO_2 ice bands that will be slightly weaker and have weaker wings. Examination of Figure 3 of Gerakines et al. (1999) suggests that subtraction of 580 K CO_2 gas, rather than 250 K CO_2 gas, would result in their same ice analogs providing an even better fit to the astronomical data in the low-frequency wing of the CO_2 ice feature in AFGL 2136. The same is likely to be true of a number of their other fits, particularly to AFGL 2591, and possibly AFGL 490, AFGL 4176, W3 IRS 5, and W33A.

In addition, the increased total absorption to the presence of warmer gas will result in the removal of some of the absorption originally inferred to be due to CO_2 ice, with the low-frequency CO_2 gas lobe decreasing the amount of CO_2 inferred to be in polar ices and the high-frequency CO_2 gas lobe decreasing the amount of CO_2 inferred to be in apolar ices. The best fits found by Gerakines et al. (1999) demonstrate that the majority of interstellar ice-phase CO_2 is in the polar component. Thus, the small relative decrease suggested by the presence of warmer CO_2 gas should not greatly affect their derived polar ice abundances. However, the high-frequency lobe of the warmer CO_2 gas will produce a proportionally greater fractional reduction in the absorption ascribed to the less abundant nonpolar component. This may help alleviate one of the greater puzzles of the CO_2 ice data returned by *ISO*. Current fits to the CO_2 ice band data using background field stars like Elias 16, which probe the general, quiescent dense cloud medium, indicate that virtually all the absorption along these lines of sight is due to CO_2 frozen in *polar* ices (Whittet et al. 1998; Gerakines et al. 1999). In contrast, the best fits to protostars embedded in dense clouds usually require the presence of additional small amounts of CO_2 frozen in *apolar* ices (Gerakines et al. 1999). This is exactly the *opposite* of what would be expected since CO ice band data suggest that nonpolar ices have a greater relative abundance along quiescent lines of sight (see Elsila et al. 1997), a point predicted by theoretical models. In addition, the main components of nonpolar astrophysical ices are considerably more volatile than the polar components, and they would be expected to be depleted *more* efficiently by sublimation in the vicinity of protostars, not less. Examination of the spectral fits in Gerakines et al. (1999) suggests that the presence of CO_2 gas that is warmer than previously assumed would decrease, and perhaps eliminate, the need for a nonpolar component to fit the CO_2 ice feature seen toward many embedded protostars, thereby potentially eliminating the apparent inconsistency between the inferred relative abundances of polar and nonpolar ices between protostellar and general cloud environments.

5.3. *Strategies for the Future Detection of Interstellar N_2-bearing Ices*

The efforts outlined above, while placing the first significant constraints on the abundance and nature of N_2 in interstellar ices, have only resulted in the determination of upper limits. Direct detections of N_2 in interstellar ices will require improvements over the current effort. A number of important criteria will have to be met if future efforts are to lead to the detection of interstellar N_2. First, and most obvious, the relative weakness of the 2328 cm^{-1} N_2 band (even when it is enhanced by molecular interactions) indicates that any future detection of N_2 will require spectra with very high S/N. In addition, the detection of interstellar N_2 will be greatly simplified by searching for it along lines of sight that suffer from a minimum of interference from other molecular bands. Ideally, one would prefer lines of sight that do not produce a saturated CO_2 ice band near 2345 cm^{-1} and that do not contain significant column densities of gas-phase CO_2, especially warm CO_2. In the case of utilizing background field stars as probes of the quiescent portions of clouds, it would be best to avoid using stars with photospheric absorption features, particularly M stars whose photospheric CO greatly complicates the search for N_2. Everything considered, it would probably be "easiest" to detect interstellar N_2 using background field stars since such lines of sight probe quiescent cloud regions that are predicted to be richer in apolar ices and should suffer from fewer problems with gas-phase CO_2. That being said, searches for N_2 toward embedded protostars, while being more difficult, are still of great interest as they probe a unique astrophysical environment in which interstellar ices are rapidly evolving.

Ultimately, it will also be desirable to obtain high-quality spectra of the probe stars across the entire 4000–500 cm^{-1} (2.5–20 μm) spectral range. Of particular importance is the 680–620 cm^{-1} (14.7–16.1 μm) region, as the unresolved Q-branch of the ν_2 CO_2 band at 668 cm^{-1} (14.97 μm) provides a very useful constraint on the contributions of gas-phase CO_2 to the N_2 band position. Once the interstellar N_2 band is detected, greater spectral coverage will be especially important. Since the strength of the N_2 ice band depends so critically on its molecular neighbors, it will be difficult to constrain the actual N_2 abundance implied by any detected band without a good understanding of what other molecules may be present in the ice.

Finally, this area would obviously benefit from additional theoretical modeling to understand better the expected abundances of N_2 in interstellar ices and how these abundances relate to local cloud conditions and previous evolutionary history. Of particular utility would be models that predict not only the abundances of N_2 but also the iden-

tities and abundances of their most likely molecular neighbors within the resulting ices.

5.4. *Molecular Nitrogen in the Solar System*

Both Pluto and Neptune's satellite Triton are known to have N_2-rich ices on their surfaces as evidenced by the first overtone of the N_2 stretching fundamental near 4656 cm^{-1} (2.148 μm). The surface ices of these objects also contain CO, CH_4, H_2O, and, in the case of Triton, CO_2 (Cruikshank et al. 1993, 1998; Owen et al. 1993; Quirico et al. 1998).

It is not clear whether the enhancements described here have any direct application to the interpretation of the spectra of the N_2-rich ices on Pluto and Triton. First, our 12 K ices contained N_2 in the low-temperature α structural form relevant to interstellar conditions. The higher temperature N_2 ices on Triton and Pluto ($T \sim 40$ K) are thought to be predominantly in the β structural form (see Grundy, Schmitt, & Quirico 1993). Enhancements to the strength of the N_2 bands may well be different for the β structural form, and there is some evidence that the enhancements may be temperature dependent. In a limited number of experiments, Bernstein & Sandford (1999) monitored the strength of the N_2 band as samples were warmed from 10 to 20, 25, and 30 K. The H_2O- and CO_2-induced enhancements of the N_2 fundamental were seen to decrease slightly with warm-up, the effect being less than 30% for CO_2 and perhaps as much as 50% for H_2O. Additional experiments will be required to quantify this effect better as a function of sample composition.

Second, N_2 on Pluto and Triton has been identified via the first overtone of the N_2 stretching fundamental near 4656 cm^{-1} (2.148 μm). Our data only address enhancements of the fundamental, not its overtone. In a limited number of cases, Bernstein & Sandford (1999) were able to detect the N_2 overtone band near 4656 cm^{-1} in the spectra of their binary ices. Several samples with N_2/H_2O ratios between 10 and 20 were found to produce overtones having strengths of between 2.7×10^{-23} and 3.9×10^{-23} cm $molecule^{-1}$, values that are enhanced relative to those reported for pure N_2 (Bohn et al. 1994) by *at most* a factor of 2, whereas the fundamentals in these samples are enhanced by factors of about 8. Similarly, overtones seen in a few $N_2/CO_2 = 20/1$ and $N_2/CO_2 = 5/1$ samples yield *maximum* strengths of 4.2×10^{-22} and 1.4×10^{-21} cm $molecule^{-1}$, respectively. These correspond to enhancements of less than a factor of about 20 and 70 for the overtones, while the fundamentals are enhanced by factors of about 110 and 660, respectively. Thus, it appears that the N_2 overtone may be less enhanced by the presence of H_2O and CO_2 than is the fundamental. Additional spectral measurements with higher S/N in the 4700–4600 cm^{-1} region will be needed to quantify this behavior better.

Finally, it is not clear that the N_2, CO_2, and H_2O in the ices on these bodies are in contact with each other at the molecular level. Current physical and spectral evidence suggests that the CH_4 and CO are mostly or entirely frozen in the N_2 ices, while the H_2O and CO_2 may be spatially segregated (Cruikshank et al. 1998; Quirico et al. 1998). Thus, the H_2O and CO_2 may not enhance the strength of the nitrogen features because they may not be in physical contact with the N_2.

Thus, the issue of whether other molecules produce enhancements of the absorption and reflection bands of N_2 in the spectra of Pluto and Triton will require additional laboratory studies that focus on conditions more relevant to these planetary environments.

6. CONCLUSIONS

The position, profile, and strength of the 2328 cm^{-1} $N{\equiv}N$ fundamental stretch of N_2 in ices are relatively insensitive to the presence of CO, CH_4, and O_2. However, the strength of this feature is significantly increased in the presence of NH_3, H_2O, or CO_2. The extent of the enhancement is dependent on the guest molecule and its concentration. At high concentrations, NH_3, H_2O, and CO_2 can lead to enhancement factors as high as 40, 80, and 1400, respectively.

Both theoretical models of interstellar ice mantle composition and direct observation of interstellar ices suggest that N_2 is likely to be abundant in dense molecular clouds. These same interstellar ices are also expected to contain NH_3, H_2O, and CO_2, implying that the N_2 fundamental near 2328 cm^{-1} should be significantly enhanced in the spectra of interstellar ices. The expected enhancements relative to pure N_2 span the range from a minimum factor of $\sim$30 to a maximum factor of over 1000, the actual value depending on the history and composition of the ice. Such enhancements significantly improve the possibility of direct detection of N_2 in interstellar ices but will make the interpretation of column densities of any N_2 detected more difficult.

Analysis of astronomical spectra probing dense cloud materials along lines of sight toward a protostellar object and a background field star yields upper limits for the abundance of interstellar N_2 ice that are just beginning to constrain interstellar grain models and the composition of possible N_2-bearing interstellar ices. The current upper limits indicate that N_2 cannot be present in CO_2-rich ices unless its abundance is lower than that predicted by models. None of the current upper limits preclude the theoretically predicted range of N_2 abundances in "typical" environments for ices in which the N_2 band is either unenhanced or enhanced only by the presence of NH_3 or H_2O.

If N_2-bearing ices are to be detected in the future, the search will require very high S/N spectra of stars that do not contain strong photospheric absorption bands (especially due to photospheric CO) and that do not probe lines of sight having saturated CO_2 ice bands. Emphasis should be placed on background stars rather than embedded protostars since field stars will probe lines of sight that (1) are likely to have formed larger relative concentrations of apolar, N_2-bearing ices; (2) will have considerably less spectral contamination by gas-phase CO_2; and (3) should suffer less N_2 ice depletion by sublimation.

Since the strength of the N_2 ice band depends so critically on molecular neighbors, it will be difficult to constrain the actual N_2 abundance implied by any detected band without a good understanding of what other molecules are present in the ice. In this vein, additional theoretical modeling designed to understand better the expected abundances of N_2 in interstellar ices and the identities and abundances of their most likely molecular neighbors within the resulting ices would be particularly useful.

Finally, the lines of sight toward protostars embedded in interstellar dense clouds may contain absorption contributions from modest amounts of relatively warm CO_2 gas. The presence of this gas may help resolve several puzzles

associated with the previously derived gas/solid CO_2 ratios and the relative abundances of polar and nonpolar ices toward these objects. In particular, the presence of warm CO_2 gas may mitigate the past apparent need for an increased contribution from CO_2 in apolar ices in protostellar regions relative to the general cloud medium, a finding that was the opposite of what would be expected. In addition, the presence of some warm CO_2 gas raises the derived gas/solid CO_2 ratios along these lines of sight to values that are more in keeping with those of other molecules and the relative volatility of CO_2.

This work was supported by NASA grants 344-38-12-04 (Exobiology), 344-37-44-01 (Origins of Solar Systems), and 399-20-61 (Long Term Space Astrophysics). The authors are grateful for useful discussions with D. Cruikshank, Eliot Young, Perry Gerakines, and Pascale Ehrenfreund, excellent technical support from R. Walker, and the helpful review of an anonymous referee. We also acknowledge IA[3] and OSIA, joint developments of the SWS consortium. Contributing institutes are SRON, MPE, KUL, and the ESA Astrophysics Division. The *ISO* Spectral Analysis Package (ISAP) is a joint development by the LWS and SWS Instrument Teams and Data Centers. Contributing institutes are CESR, IAS, IPAC, MPE, RAL, and SRON.

REFERENCES

Bernstein, M. P., & Sandford, S. A. 1999, Spectrochim. Acta, 55, 2455
Bernstein, M. P., Sandford, S. A., & Allamandola, L. J. 1997, ApJ, 476, 932
———. 2000, ApJ, 542, 894
Bohn, R. B., Sandford, S. A., Allamandola, L. J., & Cruikshank, D. P. 1994, Icarus, 111, 151
Brown, P. D., & Charnley, S. B. 1990, MNRAS, 244, 432
Caselli, P., Hasegawa, T. I., & Herbst, E. 1998, ApJ, 495, 309
Cruikshank, D. P., Roush, T. L., Owen, T. C., Geballe, T. R., de Bergh, C., Schmitt, B., Brown, R. H., & Bartholomew, M. J. 1993, Science, 261, 742
Cruikshank, D. P., Roush, T. L., Owen, T. C., Quirico, E., & de Bergh, C. 1998, In Solar System Ices, ed. B. Schmitt et al. (Dordrecht: Kluwer), 655
de Graauw, T., et al. 1996a, A&A, 315, L49
———. 1996b, A&A, 315, L345
d'Hendecourt, L. B., Allamandola, L. J., & Greenberg, J. M. 1985, A&A, 152, 130
Ehrenfreund, P., Boogert, A. C. A., Gerakines, P. A., Tielens, A. G. G. M., & van Dishoeck, E. F. 1998a, A&A, 328, 649
Ehrenfreund, P., Dartois, E., Demyk, K., & d'Hendecourt, L. 1998b, A&A, 339, L17
Elias, J. H. 1978, ApJ, 224, 857
Elsila, J., Allamandola, L. J., & Sandford, S. A. 1997, ApJ, 479, 818
Gerakines, P. A., et al. 1999, ApJ, 522, 357
Goorvitch, D. 1994, ApJS, 95, 535
Grim, R. J. A., & Greenberg, J. M. 1987, ApJ, 321, L91
Grundy, W. M., Schmitt, B., & Quirico, E. 1993, Icarus, 105, 254
Hasegawa, T. I., Herbst, E., & Leung, C. M. 1992, ApJS, 82, 167
Hudgins, D. M., Sandford, S. A., Allamandola, L. J., & Tielens, A. 1993, ApJS, 86, 713
Irvine, W. M. 1998, Origins of Life and Evolution of the Biosphere, 28, 365
Lacy, J. H., Baas, F., Allamandola, L. J., Persson, S. E., McGregor, P. J., Lonsdale, C. J., Geballe, T. R., & van der Bult, C. E. P. 1984, ApJ, 276, 533
Lacy, J. H., Faraji, H., Sandford, S. A., & Allamandola, L. J. 1998, ApJ, 501, L105
Mitchell, G. F., Maillard, J.-P., Allen, M., Beer, R., & Belcourt, K. 1990, ApJ, 363, 554
Myers, P. C., & Benson, P. J. 1983, ApJ, 266, 309
Owen, T. C., et al. 1993, Science, 261, 745
Palumbo, M. E., Pendleton, Y. J., & Strazzulla, G. 2000a, ApJ, 542, 890
Palumbo, M. E., Strazzulla, G., Pendleton, Y. J., & Tielens, A. G. G. M. 2000b, ApJ, 534, 801
Pendleton, Y. J., Tielens, A. G. G. M., Tokunaga, A. T., & Bernstein, M. P. 1999, ApJ, 513, 294
Quirico, E., Doute, S., Schmitt, B., de Bergh, C., Cruikshank, D., Owen, T., Geballe, T., & Roush, T. 1998, Icarus, 139, 159
Rothman, L. S., et al. 1998, J. Quant. Spectrosc. Radiat. Transfer, 60, 665
Sandford, S. A. 1996, Meteoritics and Planetary Science, 31, 449
Sandford, S. A., & Allamandola, L. J. 1990, ApJ, 355, 357
———. 1993, ApJ, 417, 815
Sandford, S. A., Allamandola, L. J., Tielens, A. G. G. M., & Valero, G. J. 1988, ApJ, 329, 498
Smith, R. G., Sellgren, K., & Brooke, T. Y. 1993, MNRAS, 263, 749
Tegler, S. C., Weintraub, D. A., Allamandola, L. J., Sandford, S. A., Rettig, T. W., & Campins, H. 1993, ApJ, 411, 260
Tegler, S. C., Weintraub, D. A., Rettig, T. W., Pendleton, Y. J., Whittet, D. C. B., & Kulesa, C. A. 1995, ApJ, 439, 279
Teixeira, T. C., Devlin, J. P., Buch, V., & Emerson, J. P. 1999, A&A, 347, L19
Teixeira, T. C., Emerson, J. P., & Palumbo, M. E. 1998, A&A, 330, 711
Tielens, A. G. G. M., & Hagen, W. 1982, A&A, 114, 245
Tielens, A. G. G. M., Tokunaga, A. T., Geballe, T. R., & Baas, F. 1991, ApJ, 381, 181
van Dishoeck, E. F., Blake, G. A., Draine, B. T., & Lunine, J. I. 1993, in Protostars and Planets III, ed. E. H. Levy & J. I. Lunine (Tucson: Univ. Arizona Press), 163
van Dishoeck, E. F., et al. 1996, A&A, 315, L349
Whittet, D. C. B., et al. 1996, A&A, 315, L357
———. 1998, ApJ, 498, L159
Willner, S. P., et al. 1982, ApJ, 253, 174